

# RSC Advances

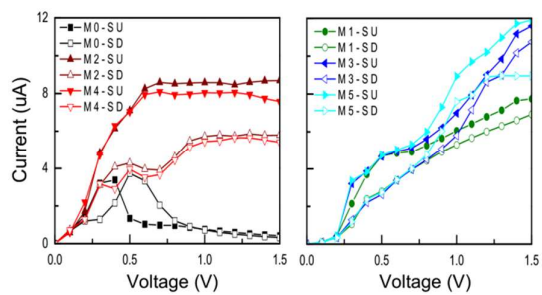


This is an *Accepted Manuscript*, which has been through the Royal Society of Chemistry peer review process and has been accepted for publication.

*Accepted Manuscripts* are published online shortly after acceptance, before technical editing, formatting and proof reading. Using this free service, authors can make their results available to the community, in citable form, before we publish the edited article. This *Accepted Manuscript* will be replaced by the edited, formatted and paginated article as soon as this is available.

You can find more information about *Accepted Manuscripts* in the [Information for Authors](#).

Please note that technical editing may introduce minor changes to the text and/or graphics, which may alter content. The journal's standard [Terms & Conditions](#) and the [Ethical guidelines](#) still apply. In no event shall the Royal Society of Chemistry be held responsible for any errors or omissions in this *Accepted Manuscript* or any consequences arising from the use of any information it contains.



Spin-dependent transport properties can be modulated by the oddity of the side alkene chain in defective ZGNR junction.

# Control of electronic transport in nanohole defective zigzag graphene nanoribbon by means of side alkene chain

Yun Zou<sup>1</sup>, Mengqiu Long<sup>1,2,\*</sup>, Mingjun Li<sup>1</sup>, Xiaojiao Zhang<sup>1</sup>, Qingtian Zhang<sup>2,†</sup>, and Hui Xu<sup>1</sup>

<sup>1</sup>*Institute of Super-microstructure and Ultrafast Process in Advanced Materials, School of Physics and Electronics, Central South University, Changsha 410083, China*

<sup>2</sup>*Department of Physics and Materials Science, City University of Hong Kong, Hong Kong, China.*

## Abstract

Using the nonequilibrium Green function formalism combined with density functional theory, we studied the electronic transport properties of nanohole defective zigzag graphene nanoribbon (ZGNR) junction. A side alkene chain is connected to the edge of the defective ZGNR in the scattering region. We find that the transport properties of the defective ZGNR junction are strongly dependent on the oddity of the number of carbon atoms for the side alkene chain. The side chain can switch on (even) and off (odd) the transport channel of our proposed junction. It is found that the transmissions for the side chains with an even number of carbon atoms are around  $2G_0$ , but they are around  $1G_0$  for the side chains with an odd number of carbon atoms. The origin of this peculiar behavior is analyzed as due to the electronic states at the edge of the defective ZGNR which are modulated by the side-chain length. Our theoretical study shows that it is feasible to control the conduction of ZGNR by changing the side-chain length via external modulations such as chemical methods, which may stimulate experimental investigations in the future.

**Keyword:** Zigzag graphene nanoribbon, nanohole defect, density functional theory, side alkene chain

---

\* mqlong@csu.edu.cn

† qtzhang@mail.ustc.edu.cn

## Introduction

Electron transport through a graphene nanoribbon (GNR) junction has recently received considerable experimental<sup>1-3</sup> and theoretical<sup>4-7</sup> attentions. Different from bulk graphene, GNRs have energy gaps, which make them suitable for the realization of electronic devices<sup>8</sup>. Until now, many electronic devices have been realized in the GNR nanostructures, such as field-effect transistors (FET)<sup>9-11</sup>, switches<sup>12, 13</sup>, gas molecular sensors<sup>14, 15</sup>, spintronic devices<sup>16, 17</sup> and rectifiers<sup>18, 19</sup>. According to the geometry of the edge, GNRs can be divided into two kinds: Armchair GNR (AGNR) and Zigzag GNR (ZGNR). In case that the spin effect is disregarded, previous studies show that ZGNRs are expected to be metallic regardless of their width whereas AGNRs can be metallic or semiconducting depending on their width<sup>20</sup>. Among them, ZGNRs have attracted much more attentions due to the unique edge states and edge magnetism. Owing to the potential applications of the ZGNRs in nanosized spintronic devices, a number of researches have been done, and the zigzag-edge states are shown to be modified by doping atoms, side groups, and defects at the edges<sup>21, 22</sup>.

Generally, defects and side groups in GNRs can affect the magnetic and electrical properties in unexpected ways, which are commonly used to modulate artificially the electronic structures of GNRs. Punching nanoholes on graphene could increase the band gap of graphene and make it change from the semimetal to semiconductor<sup>23-25</sup>. Moreover, theoretical studies showed that the molecular electronic transport properties of a ZGNR are strongly dependent on the edge states<sup>26</sup>, introducing side groups is an effective way for modulating of edge structure ZGNRs, providing us a

method to control the transport properties of ZGNRs devices. Side chains modulation can bring many novel properties such as Fano effect<sup>27, 28</sup> and the standing wave effect<sup>29, 30</sup>. Moreover, the electronic transport properties can also be controlled through chemical conformational modification of side chains to aromatic molecules<sup>31-33</sup>.

But up to now, as we know, there is no literature to report the control of electronic transport properties by means of side-chain length in defective graphene nanoribbons. In fact, the GNRs are an important nanostructures for developing nano-devices in the future, and the nanohole defects and side chain are effective methods for modulating the electronic structures of ZGNRs. Thus, it is very necessary to study the electronic transport behaviors in nanohole-defected ZGNRs with side chains. In this paper, we design a nanohole in ZGNR and study the spin-dependent transport properties of the defective ZGNR device with different length of side alkene chain. The goal of this work is to improve the existing understanding of a mechanism to control the current in the GNRs-based molecular electronic devices.

## Models and methods

We study the spin-dependent transport properties of a nanohole defective ZGNR with a side alkene chain. As shown in Fig. 1, six carbon atoms are removed from the scattering region in the zigzag graphene nanoribbon, and the scattering region with a nanohole in the center forms a 18-membered carbon ring, which follows the molecular structure of an Annulene. Previous studies have shown that the geometric structure of Annulene is stable and it has a good electrical conductivity<sup>34</sup>, so it is interesting for us to study the transport properties. A side alkene chain  $(\text{CH})_n\text{H}$  is linked to the ZGNR, where  $n$  is an integer number ( $n = 0, 1, 2, \dots$ ). In our numerical

simulation, six systems with  $n = 0, 1 \dots 5$  are considered, for example, when  $n = 2$ , the side chain is  $C_2H_3$  (M2,  $n = 2$ ). In this work, all calculations are performed by Atomistix ToolKit (ATK) package<sup>35-37</sup>, in which the nonequilibrium Green's function formalism (NEGF) and density functional theory (DFT) are implemented. A cutoff energy of 150 Ry and a Monkhorst–Pack  $k$ -mesh of  $1 \times 1 \times 100$  with a convergence criterion of  $10^{-6}$  eV are chosen to achieve the balance between calculation efficiency and accuracy. We have checked total energy with different cutoff energies for our systems, and we found that 150 Ry is a suitable value for our numerical calculation. That is why 150 Ry has been employed in many previous studies<sup>38, 39</sup>. Moreover, a double Zeta plus polarized (DZP) basis set is adopted for electron wave function. The NEGF-DFT self-consistency is controlled by a numerical tolerance of  $4 \times 10^{-5}$  eV. And also, the double contour integral has been used to integrate the Green's function in the real axis, the convergence is  $10^{-5}$  eV, and point density is 0.002 eV have been used in the integral. The vacuum layers between two ribbons along the  $x$  and  $y$  directions (defined in Fig. 1) are 15 Å to avoid the artificial Coulomb interactions between the contents in two neighboring cells. To obtain accurate results, all the systems after functionalization with a side chain have been performed geometry optimization until the force on each atom is less than 0.05 eV/Å. The spin-polarized current through the system is calculated using the Landauer–Büttiker formula<sup>40</sup>,

$$I_{\sigma}(V_b) = \frac{e}{h} \int_{\mu_R(V_b)}^{\mu_L(V_b)} \left\{ T_{\sigma}(E, V_b) [f_L(E, V_b) - f_R(E, V_b)] \right\} dE \quad (1)$$

where  $e$  is the electron charge,  $h$  is the Planck's constant, and  $T_{\sigma}$  is the transmission of an electron with spin  $\sigma$ .  $f_{L(R)}(E, V_b)$  is the Fermi-Dirac distribution function of the left (right) electrode, and the difference of the chemical potentials between the left and right electrodes is  $\mu_L(V_b) - \mu_R(V_b) = eV_b$ , where  $V_b$  denotes the external bias voltage.  $T_{\sigma}$  can be obtained from the equation,

$$T_{\sigma}(E, V_b) = Tr \left[ \text{Im} \left\{ \sum_{L_{\sigma}}^r (E, V_b) \right\} G_{\sigma}^r(E, V_b) \times \text{Im} \left\{ \sum_{R_{\sigma}}^r (E, V_b) \right\} G_{\sigma}^a(E, V_b) \right] \quad (2)$$

where  $G^r$  ( $G^a$ ) is the retarded (advanced) Green's function matrix, and  $\Sigma_L^r$  ( $\Sigma_R^r$ ) is the retarded self-energy matrix for the left (right) electrode.

## Results and discussions

Fig. 2 presents the transmission spectra of nanohole defective ZGNRs for side chains with different number of carbon atoms ( $n = 0, 1 \dots 5$ ) under zero bias. Generally, there are two different spin configurations for the ZGNR, parallel (P) and antiparallel (AP) spin configurations. The spin-up and spin-down electron in transmission spectra of ZGNR are split when the electrodes are in P spin configuration, while they are degenerate when the electrodes are in AP spin configuration<sup>41, 42</sup>. Since the behavior of the spin splitting on ZGNR may have more interesting potential applications on spintronics devices, the P spin configuration of the ZGNR has been chosen in our calculations. It is noted that the transmission coefficients at the Fermi level (FL) have still high values even if ZGNR is punched. We can find that the transmission peaks near FL for the side chains with an even number of carbon atoms are around  $2G_0$  ( $G_0 = e^2/h$  is the quantum conductance), however, they are around  $1G_0$  for the side chains with an odd number of carbon atoms, which means the conduction of nanohole defected ZGNRs can be modulated by the parity of their side alkene chains. For the structure under consideration, the atoms on the two edges provide the conduction channels in the scattering region, so the side chains connected to the edge atoms have evident effects on the transport properties.

To understand the different effects of side chains with an odd and even number of carbon atoms, we present the electron transmission pathways at Fermi level (0.0 eV)

under zero bias for the spin up and spin down states of M0, M1, M2, M3, M4 and M5 systems. As shown in Fig. 3, (a-l), the volume of each arrow indicates the magnitude of the local transmission between each pair of atoms, and the arrow and the color designate the direction of the electron flow. The transmission pathways  $T_{ij}$  can show us the local bond contributions to the transmission coefficient, for example, the total transmission coefficient between two parts A and B can be expressed as  $T(E) = \sum_{i \in A, j \in B} T_{ij}(E)$ . We can clearly find that the transmission pathways of our proposed systems are strongly dependent on the oddity of the number of carbon atoms for the side chain. For the case of a side chain with an even number of carbon atoms, such as  $n = 0, 2, 4$ , as shown in Figs. 3(a, b, e, f, i, j), there are two transmission pathways at the two edges of the nanoribbon, and both the spin-up and spin-down electrons can move from the left electrode to the right electrode, and they both have two conduction channels. Nevertheless, for the odd case, such as  $n = 1, 3, 5$ , as shown in Figs. 3(c, d, g, h, k, l), we can find that electrons can't pass through the edge connected to the side chain, and there is only one conduction channel on the other edge for each system.

As we know that the charge can move in the ZGNR system is because of the channels provided by the molecular orbital. The main channels for charge transport are determined by the frontier molecular orbital near the Fermi energy, which are called HOMO (the highest occupied molecular orbital) and LUMO (the lowest occupied molecular orbital). To further understand the transmission spectra presented in Fig. 2, we plot the frontier molecular orbital of our proposed structure in Fig. 4.

Since the spin-dependent transport properties of our proposed systems are strongly dependent on the oddity of the number of carbon atoms for the side chain, we only present the numerical results for three ZGNR devices with  $n = 0, 4, 5$  due to the space limitation. Considering the fact that HOMO is closer to FL than LUMO and mainly contribute to the electronic transport for each device, we only show the spatial distribution of the contour map for HOMO. And also the three devices with the side chains of  $n = 0, 4, 5$  have been selected in here. It is noted in Figs. 4 (a), (c) and (e) that the spin-down HOMO states for side chains with different number of carbon atoms M0, M4, M5 are all localized. For the spin-up HOMO states, they are all delocalized, however, it is easy for us to note that there are obvious differences between structures with even number chain and odd number chain. The HOMO states for side chains with even number of carbon atoms are delocalized on the two edges of the ZGNR, but the HOMO states for side chains with odd number of carbon atoms are only delocalized one edge. Since the delocalized states contribute to the transmission of the carriers we have the differences in transmission for the structures with even number side chain and odd number side chain.

Moreover, as shown in Fig. 5, we also study the local density of states (LDOS) at Fermi level under zero bias for M0, M4, and M5. The previous studies have shown that the transport properties depend on the edge states and symmetry of ZGNRs [37, 38]. It is noted in Figs. 5 (a) and (b) that transport properties of the defective ZGNR are determined by the two edge states. For the chain with even number of carbon atoms M4, as shown in Figs. 5 (c) and (d), the LDOS are similar to M0, we have the

LDOS localized over the two edges of the defective ZGNR. However, it is different for the structures connected to a chain with odd number of carbon atoms, and we can see from Figs. 5 (e) and (f) that the LDOS are zero around the site of the upper edge that linked to the side chains. As we know, the delocalized edge states play a significant role in the electronic transport properties in defective ZGNRs, but the localized states give very little contribution to electronic transport, which corresponds to the suppressed transmission coefficient in Figs. 2(b), (d), and (e). The defective ZGNRS linked to even side chains have two transport channels, and we can see it from Figs. 5 (c) and (d) that both the channels of upside edge and downside edge are opened. But for the defective ZGNRS linked to odd chains, the channel of upside edge is closed. The analysis agree well with the results presented in Fig. 2.

In order to understand the physical mechanism of the coupling between the side alkene chain and the zigzag edge states, as shown in Fig. 6, we also present the spin dependent transmission spectra under zero bias for the side alkene chain doped non-defective ZGNR systems. There are three perfect ZGNRs for side chains with the number of carbons  $n = 0, 4, 5$  have been chosen, which are named by Z0, Z4 and Z5 for short. Comparing with the results of the defective ZGNRs systems M0, M4 and M5 in Fig. 2(a), (e) and (f), it is clearly seen that the transmission spectra in Fig.6 are strongly correlated to the non-defective and defective ZGNRs, especially at the location of their peaks. The difference is that there is an initial conductance platform about 1.0 G0 for the non-defective systems, while that is about zero for the defective systems. Thus, in the defective systems, we can see that the transmission channels are

almost contributed from the transmission peaks near the Fermi level, and transport behaviors of the defective ZGNR devices would be almost modulated by the doped side chain. Moreover, we can find the zero values of transmission coefficients at some higher energy points in Fig. 6 (b) and (c), which caused by the resonant backscattering states formed in the side chains<sup>6,21</sup>.

Furthermore, we also plot the LDOS at Fermi level as inserts in Fig. 6. We can clearly see that the distributions of the LDOS are delocalized in whole scattering region for each system. Only very little edge state around the side chain is suppressed in Z5 rather than Z0 and Z4, so it is impossible to observe the dependence of transport properties on the oddity of the number of carbon atoms for the side alkene chain in side alkene chain doped non-defective ZGNR systems. Thus, the side chains could play a more prominent role on the transport properties of the nanohole defective ZGNRs than that of the perfect ones.

In addition, for a further insight into the spin-dependent transport properties of the nanohole defected ZGNRs devices, we present the current-voltage ( $I$ - $V$ ) curves of all systems in Fig. 7. The  $I$ - $V$  curves for the systems with even side chains and odd side chains are shown in Fig. 7(a) and Fig. 7(b), respectively. We can know from the Fig. 6 that the currents of all systems in the area of low bias increase quickly with the increase of the bias, which shows the conductive properties of metals. And the current of systems with even chains are bigger than those of with odd chains, and which can be explained by the transmission shown in Fig. 2. This is because the transmissions for the side chains with an even number of carbon atoms are larger than the

transmission for the side chains with an odd number of carbon atoms. With the increase of bias, comparing Fig. 7(a) with Fig. 7(b), it is found that the currents of odd chains and even chains present completely different changing laws. In the region of bias 0.2 to 1.0 V, the currents for side chains with an even number of carbon atoms almost remain the same. The currents for side chains with an odd number of carbon atoms are completely different, and it is noted that the relation between currents and the gate voltages agrees well with the Ohm Law. Furthermore, we also can find the currents of spin-up and spin-down are split with the increase of the bias for each system, which means that the systems we proposed can appear spin undegenerated transport behaviors. And the nanohole defected ZGNRs devices would have potential applications in the field of spintronics. More interestingly, as shown in the  $I$ - $V$  curves of M0, when  $V_b > 0.4$  V for spin-up state, and  $V_b > 0.5$  V for spin-down state, the spin-up and spin-down currents are decreased by the increasing of the bias, and the obvious negative differential resistance (NDR) behaviors can also be observed for both the spin-up and spin-down states of M0. From the above results, we can know that different transport behaviors of the nanohole defective ZGNRs originate from different electronic states at the edge of the defective ZGNR which can be modulated by the side alkene chains.

Due to the current is determined by the values of  $T(E, V_b)$  in the bias window (Eq.1), to further understand the spin-dependent transport behaviors, take M0, M4 and M5 as examples, the spin-dependent transmission spectra as a function of the electron energy and bias are plotted in Fig. 8. At low bias, the large transmission peaks can be

observed around the Fermi level and is broadened with the increase of bias in each panel, which leads to a quick increase in the current, and the Ohmic  $I$ - $V$  curves can be found for each system under the lower bias. With the increase of bias, it is noted that the values of transmission are different between the spin-up and spin-down electrons for each system, so the spin-undegenerated transport behavior can be observed on the  $I$ - $V$  curves in Fig. 7. Especially, it is clearly seen that the transmission spectra of spin-up in Fig. 8(d) are significantly larger than that in Fig. 8(c) in a wide bias region, which results in the obvious spin-filter effects for M4. For M4 and M5, we can find that the transmission in the bias windows are increased steadily, which results in continuous growth of current in Fig. 7. However, for M0, we can clearly find that both the transmissions of spin-up and spin-down states in the bias window are reduced with the increase of bias, which results in the NDR behaviors on the  $I$ - $V$  curves in Fig. 7.

## Conclusion

In summary, using non-equilibrium Green's functions combined with the density functional theory, we have investigated the electronic transport properties of nanohole-defective ZGNRs linked to side alkene chains. Different numbers (odd or even) of carbon atoms for the side chains linked to defective ZGNR junction were considered. The calculated results show that the side alkene chains can significantly change the electronic transport behaviors of the defective ZGNRs. We find that the defective ZGNRs linked to side chains with an even number of carbon atoms are semiconductor, while the metallic can be observed for those with an odd number of carbon atoms. Our theoretical analysis shows that the substituted-odd side chains can change the

distribution of the electronic states at the edges of the nanohole defective ZGNRs and results in the peculiar transport characteristics. We find that the odd side chains generally breaks down the edge states along the same edge, which carries less current in the junction in the area. The transmission for the side chains with an odd number of carbon atoms is half of the transmission for the side chains with an even number of carbon atoms around the Fermi level. As a consequence electron transport through the molecule can be controlled either by chemically modifying the side group, or by changing the conformation of the side group. Moreover, the interesting NDR behaviors also can be observed on the proposed nanohole defective ZGNR junction. These results suggest that the edge modified ways make the graphene-based nanomaterials present more abundant electronic transport phenomena and can be useful for the design of future nanoelectronic devices.

### Acknowledgments

This work was supported by the National Natural Science Foundation of China (Grant Nos. 21103232, 61306149, and 11334014), the Natural Science Foundation of Hunan Province (No. 14JJ3026), Postdoctor Foundation of China (Nos. 2013M542130 and 2014M552145), the Hunan Postdoctoral Scientific Program (2013RS4048), the Fundamental Research Funds for the Central Universities of Central South University (2013zzts158) and Hunan Key Laboratory for Super-microstructure and Ultrafast Process.

### References

1. P. Neugebauer, M. Orlita, C. Faugeras, A. L. Barra and M. Potemski, *Phys. Rev. Lett.*, 2009, 103, 136403.
2. C. X. Lian, K. Tahy, T. Fang, G. W. Li, H. G. Xing and D. Jena, *Appl. Phys. Lett.*, 2010, 96, 103109.

3. Y.-S. Shin, J. Y. Son, M.-H. Jo, Y.-H. Shin and H. M. Jang, *J. Am. Chem. Soc.*, 2011, 133, 5623-5625.
4. Y. W. Son, M. L. Cohen and S. G. Louie, *Nature*, 2006, 444, 347-349.
5. Z. Li, H. Qian, J. Wu, B.-L. Gu and W. Duan, *Phys. Rev. Lett.*, 2008, 100, 206802.
6. B. Biel, X. Blase, F. Triozon and S. Roche, *Phys. Rev. Lett.*, 2009, 102, 096803.
7. M. Q. Long, L. Tang, D. Wang, L. J. Wang and Z. G. Shuai, *J. Am. Chem. Soc.*, 2009, 131, 17728-17729.
8. F. Cervantes-Sodi, G. Csányi, S. Piscanec and A. Ferrari, *Phys. Rev. B*, 2008, 77, 165427.
9. X. Tan, H.-J. Chuang, M.-W. Lin, Z. Zhou and M. M.-C. Cheng, *J. Phys. Chem. C* 2013, 117, 27155.
10. P. B. Bennett, Z. Pedramrazi, A. Madani, Y. C. Chen, D. G. de Oteyza, C. Chen, F. R. Fischer, M. F. Crommie and J. Bokor, *Appl. Phys. Lett.*, 2013, 103, 253114.
11. M. J. Hollander, H. Madan, N. Shukla, D. A. Snyder, J. A. Robinson and S. Datta, *Appl. Phys. Exp.*, 2014, 7, 055103.
12. N. Al-Aqtash, H. Li, L. Wang, W.-N. Mei and R. F. Sabirianov, *Carbon*, 2013, 51, 102-109.
13. Y. Khatami, J. Kang and K. Banerjee, *Appl. Phys. Lett.*, 2013, 102, 043114.
14. F. M. Hossain, F. Al-Dirini and E. Skafidas, *J. Appl. Phys.*, 2014, 115, 214303.
15. C. Ritter, R. B. Muniz and A. Latge, *Appl. Phys. Lett.*, 2014, 104, 143107.
16. K. Xu and P. D. Ye, *Appl. Phys. Lett.*, 2014, 104, 163104.
17. J. Zeng, L. Z. Chen and K. Q. Chen, *Organic Electronics*, 2014, 15, 1012-1017.
18. T. Chen, X. F. Li, L. L. Wang, K. W. Luo and L. Xu, *J. Appl. Phys.*, 2014, 116, 013702.
19. S.-L. Yan, M.-Q. Long, X.-J. Zhang and H. Xu, *Phys. Lett. A*, 2014, 378, 960-965.
20. Y. Kobayashi, K.-i. Fukui and T. Enoki, *Phys. Rev. B*, 2006, 73, 125415.
21. C. Cao, L.-N. Chen, M.-Q. Long, W.-R. Huang and H. Xu, *J. Appl. Phys.*, 2012, 111, 113708.
22. C. Jiang, X.-F. Wang and M.-X. Zhai, *Carbon*, 2014, 68, 406-412.
23. W. Liu, Z. F. Wang, Q. W. Shi, J. Yang and F. Liu, *Phys. Rev. B*, 2009, 80, 233405.
24. W. Oswald and Z. Wu, *Phys. Rev. B*, 2012, 85, 115431.
25. W. Tian, Y. C. Zeng and Z. H. Zhang, *J. Appl. Phys.*, 2013, 114, 074307.
26. A. K. Manna and S. K. Pati, *J. Mat. Chem. C*, 2013, 1, 3439.
27. A. Chakrabarti, *Phys. Rev. B*, 2006, 74, 205315.
28. H. H. Fu and K. L. Yao, *J. Chem. Phys.*, 2011, 134, 054903.
29. L. Simon, C. Bena, F. Vonau, D. Aubel, H. Nasrallah, M. Habar and J. C. Peruchetti, *Euro. Phys. J. B*, 2009, 69, 351-355.
30. C. Park, H. Yang, A. J. Mayne, G. Dujardin, S. Seo, Y. Kuk, J. Ihm and G. Kim, *Proc. Nat. Acad. Sci.*, 2011, 108, 18622-18625.
31. R. Stadler, *Phys. Rev. B*, 2009, 80, 125401.
32. M. Q. Long, K. Q. Chen, L. L. Wang, W. Qing, B. S. Zou and Z. Shuai, *Appl. Phys. Lett.*, 2008, 92, 243303.
33. N. Liu, Z. Q. Zheng, Y. X. Yao, G. P. Zhang, N. Lu, P. J. Li, C. Z. Wang and K. M. Ho, *J. Phys. D: Appl. Phys.*, 2013, 46, 235101.
34. S. H. Ke and W. Yang, *Nano Lett.*, 2008, 8, 3257-3261.
35. J. Taylor, H. Guo and J. Wang, *Phys. Rev. B*, 2001, 63, 245407.
36. M. Brandbyge, J. Mozos, eacute, Luis, Ordej, oacute, P. n, J. Taylor and K. Stokbro, *Phys. Rev. B*, 2002, 65, 165401.

37. J. M. Soler, E. Artacho, J. D. Gale, A. Garcia, J. Junquera, P. Ordejon and D. Sanchez-Portal, *J. Phys. Cond. Mat.*, 2002, 14, 2745-2779.
38. Y. Ni, K. Yao, H. Fu, G. Gao, S. Zhu and S. Wang, *Sci. Rep.*, 2013, 3, 1380.
39. J. Zeng, K. Q. Chen and C. Q. Sun, *Phys. Chem. Chem. Phys.*, 2012, 14, 8032-8037.
40. M. Büttiker, Y. Imry, R. Landauer and S. Pinhas, *Phys. Rev. B*, 1985, 31, 6207-6215.
41. R. Qin, J. Lu, L. Lai, J. Zhou, H. Li, Q. Liu, G. Luo, L. Zhao, Z. Gao, W. Mei and G. Li, *Phys. Rev. B*, 2010, 81, 233403.
42. W. Y. Kim and K. S. Kim, *Nature Nanotechnology*, 2008, 3, 408-412.

## Figures

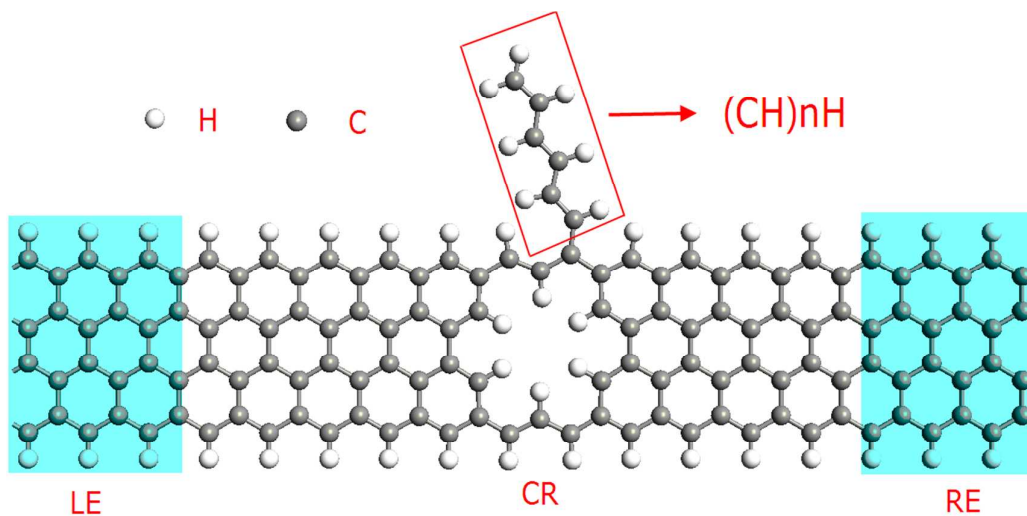


**Figure 1.** (Color online) Schematic illustration of the two-probe ZGNR system: LE, RE, and CR denote the left electrode, the right electrodes, and the central scattering region, respectively. A side chain  $(\text{CH})_n\text{H}$  is connected to the central edge of the defected ZGNR, and the edge carbon atoms are saturated with hydrogen atoms.

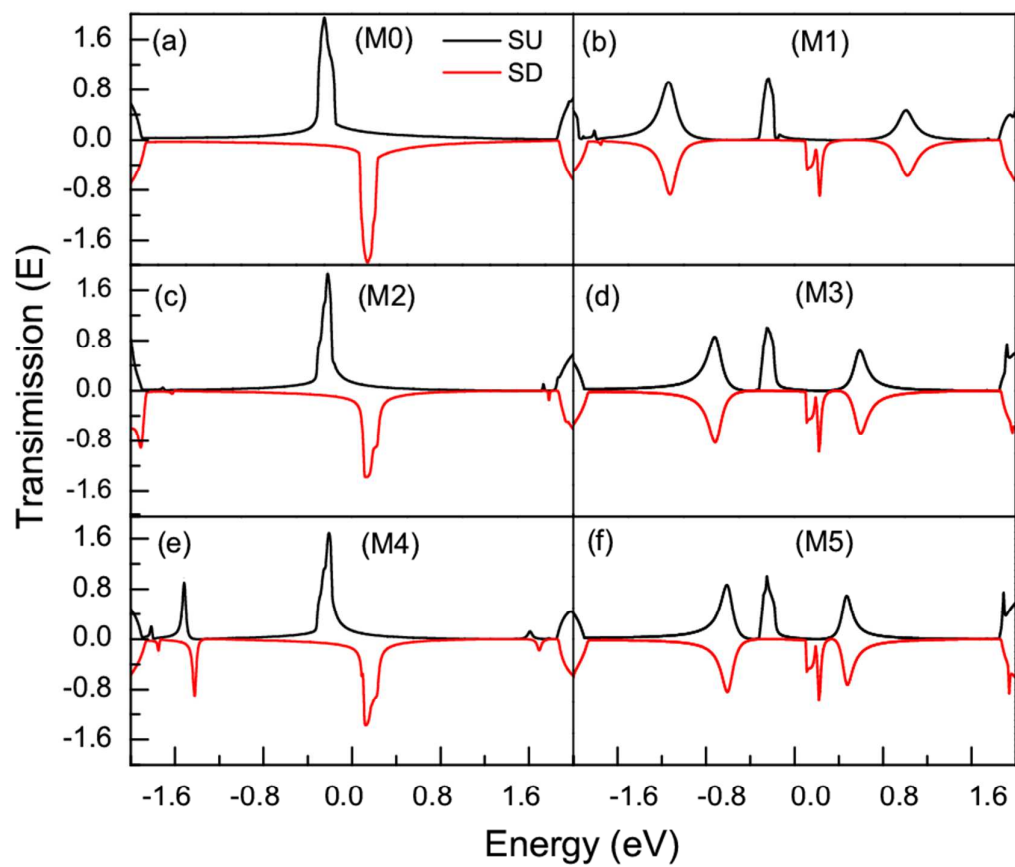


**Figure 2.** (Color online) The spin-dependent transmission spectra  $T(E, V_b)$  for all systems under the bias of zero. The Fermi level is set to zero. SU (SD) is transmission spectrum for spin-up (spin-down) electrons.

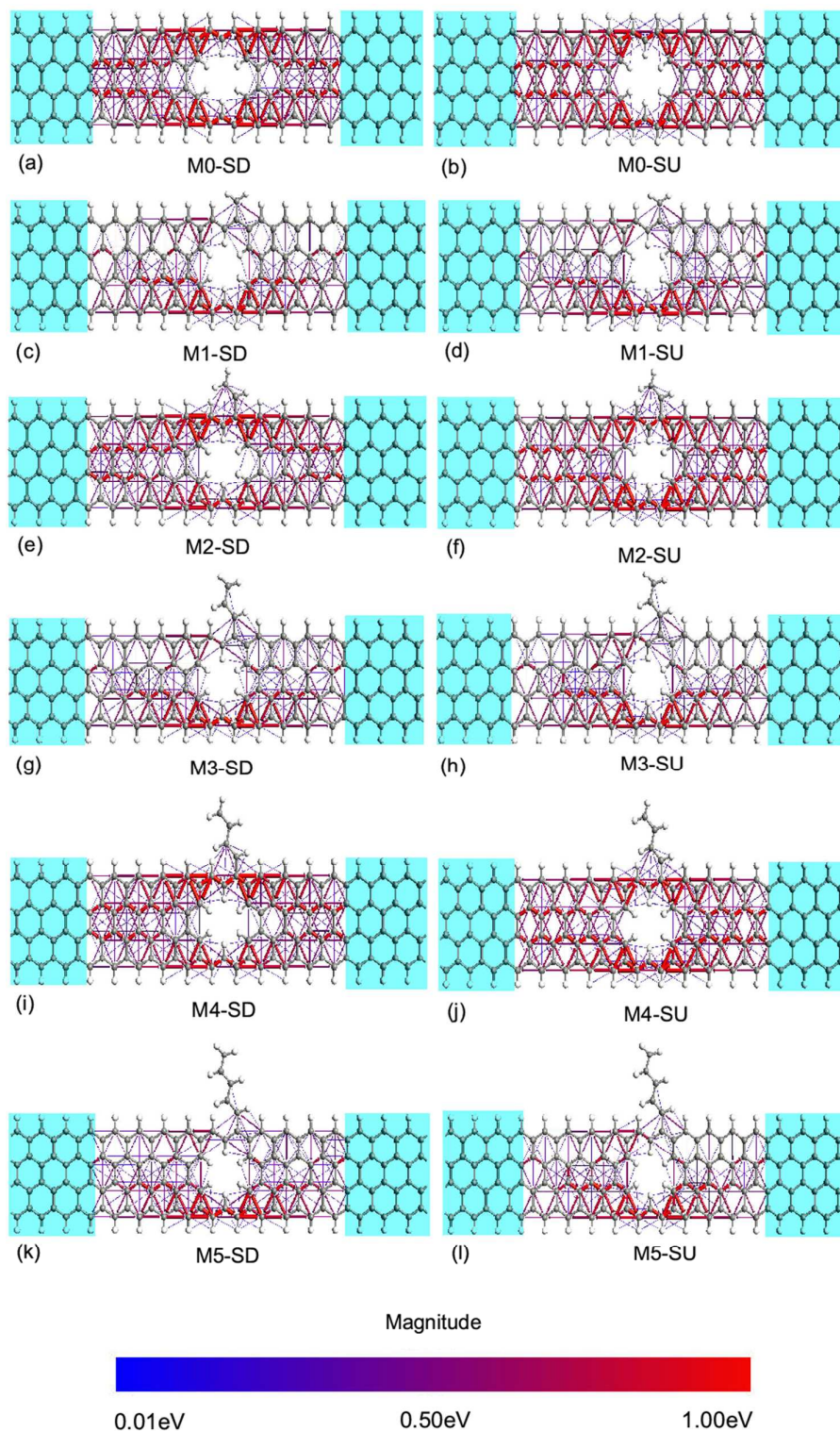


**Figure 3.** (Color online) The electron transmission pathways at Fermi level (0.0 eV) under zero bias. (a)-(l) refer to the spin up and spin down states of M0, M1, M2, M3, M4 and M5 systems, respectively.

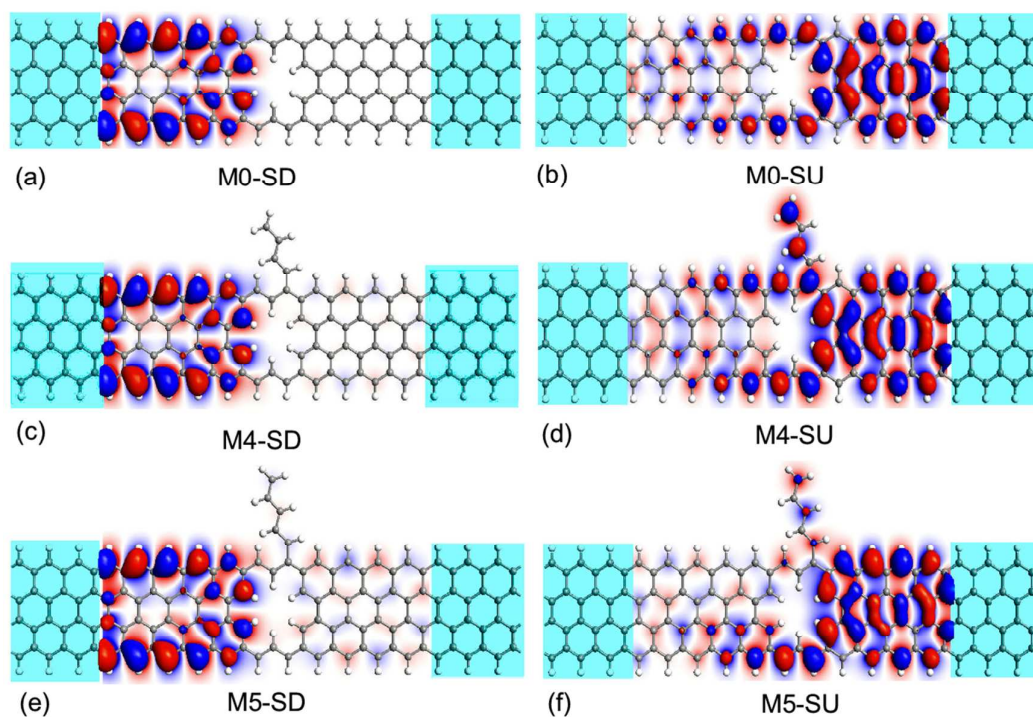


**Figure 4.** (Color online) The frontier molecular orbitals of HOMO eigenstates at 0.0 eV under zero bias. (a)-(f) the spin up and spin down states of M0, M4 and M5 systems, respectively. The isovalue is 0.05 a.u. Red and blue are used to indicate the positive and negative signs of the wavefunctions, respectively.

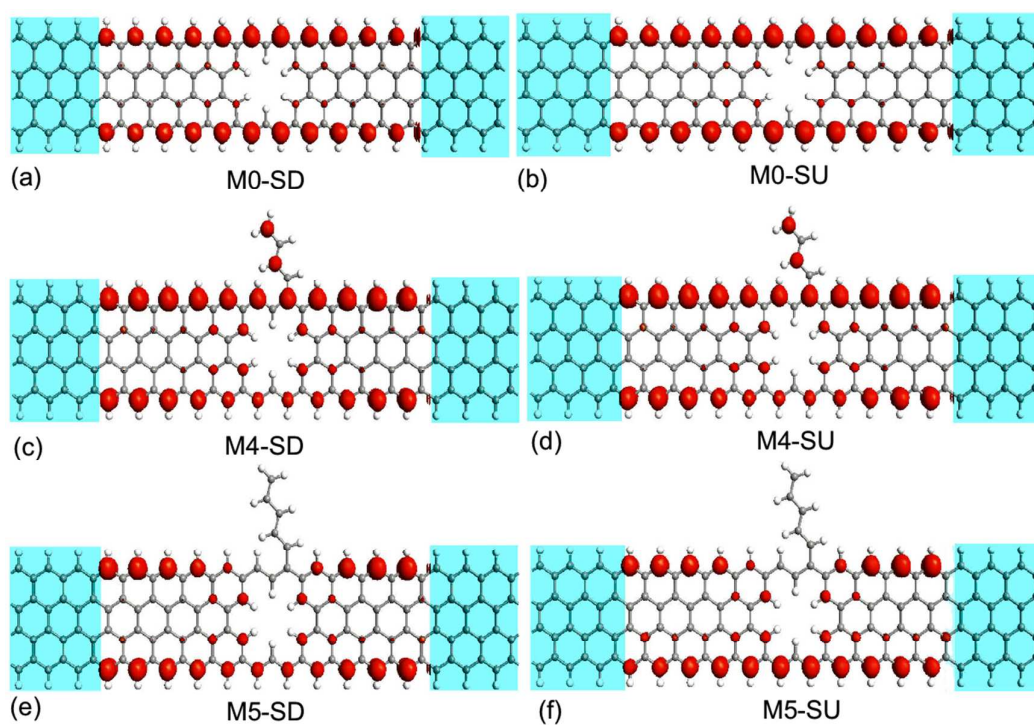


**Figure 5.** (Color online) The spin-dependent LDOS at Fermi level under zero bias. (a)-(f) the distributions of the LDOS plot at the isovalue of  $0.1e$  for the spin up and spin down states of M0, M4 and M5 systems, respectively.

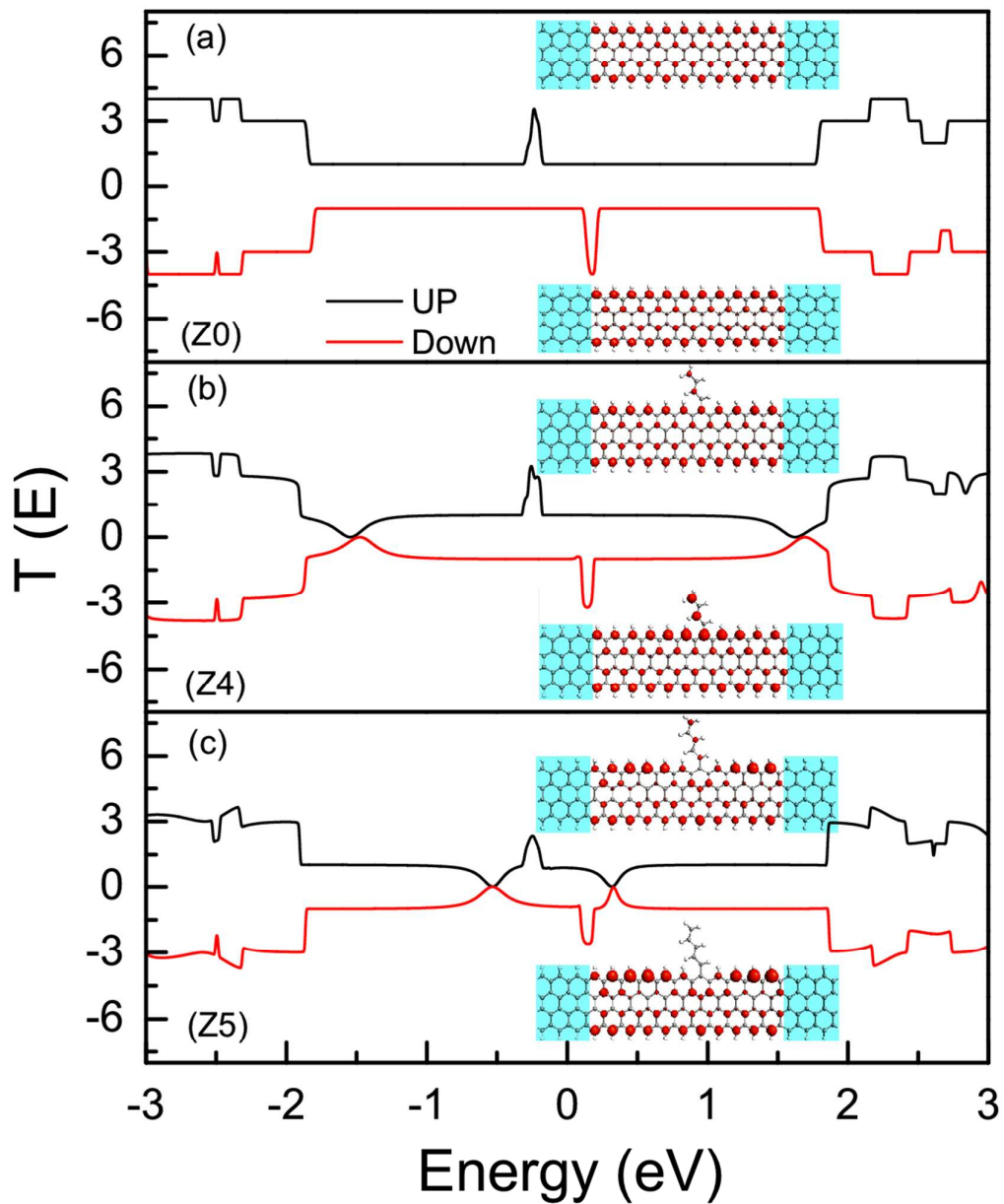


**Figure 6.** The spin-dependent transmission spectra of the non-defective 4ZGNR under zero bias. (a)-(c) Z0, Z4 and Z5 refer to the systems with different number of carbons in side chains as  $n=0, 4, 5$ , respectively. The inserts indicate the corresponding spin-dependent LDOS at Fermi level under zero bias, and the isovalue is 0.1e.

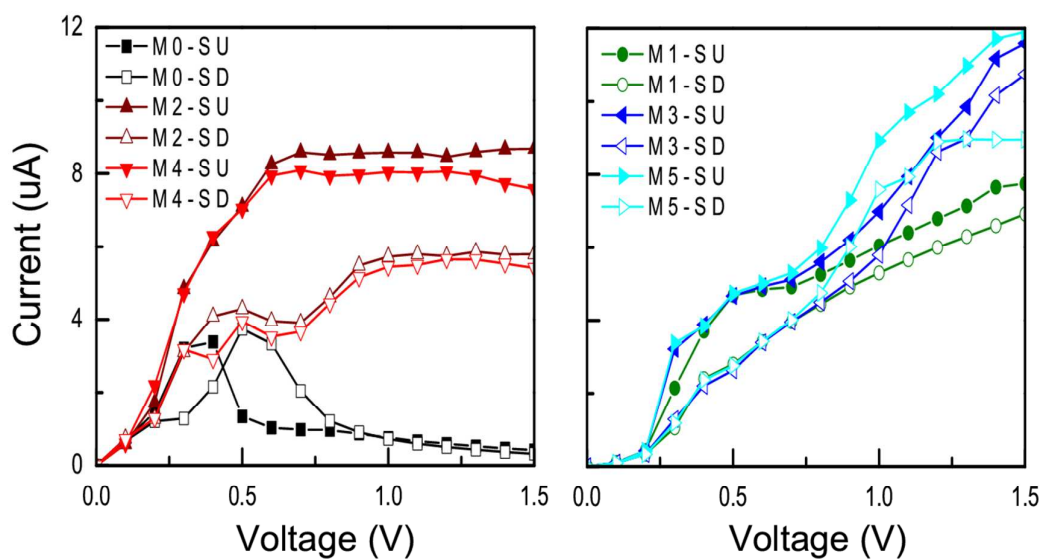


**Figure 7.** (Color online) The currents as function of applied bias voltage for the systems with different side alkene chains: (a) all even and (b) all odd.

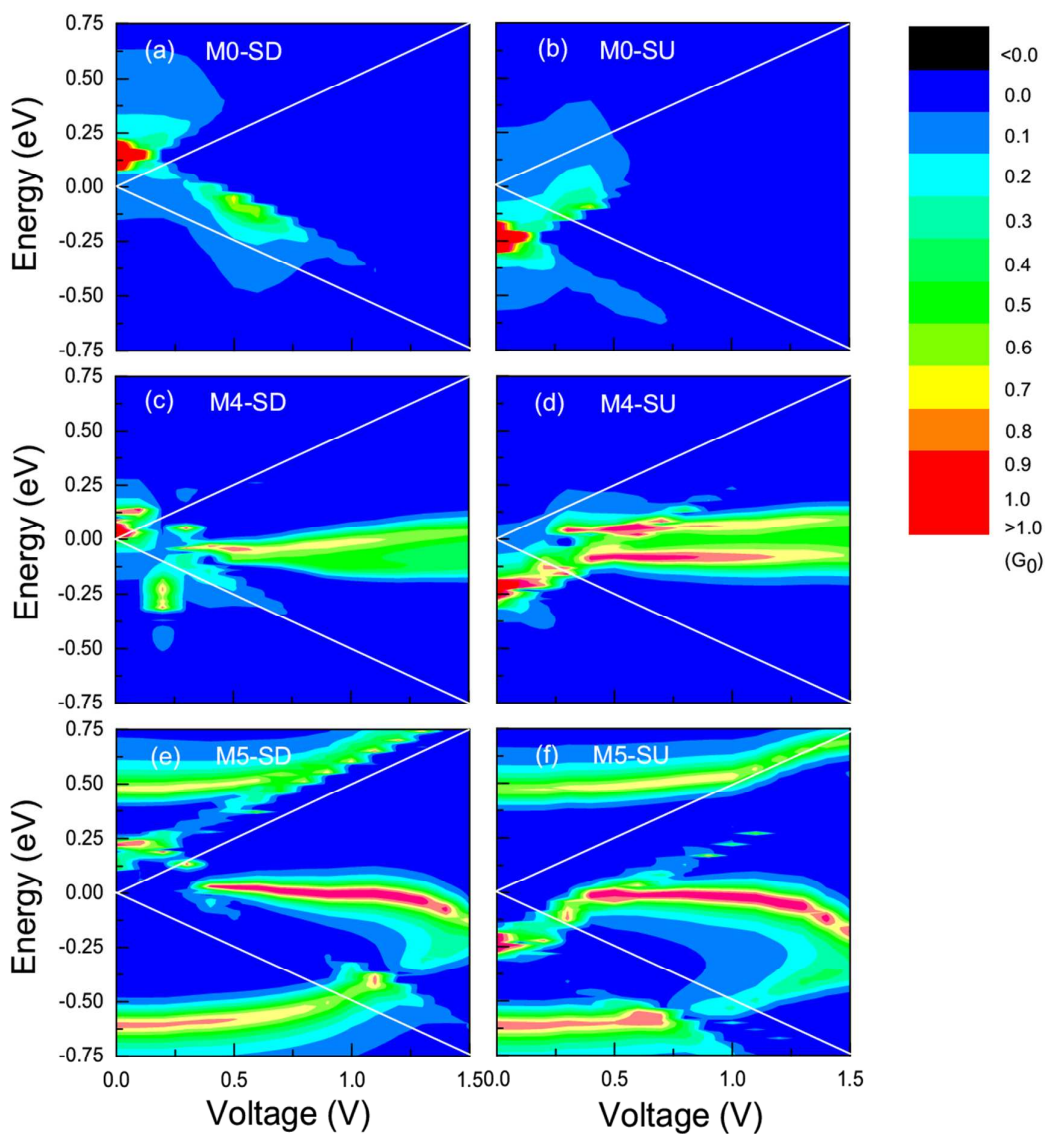


**Figure 8.** (Color online) Calculated transmission spectra as a function of electron energy  $E$  and bias for spin-down and spin-up states of M0, M4 and M5. The region between the white solid lines is referred to bias window.